BREAKUP OF VARIOUS LIQUID JETS BY SHOCK WAVES AND APPLICATIONS TO RESONANT COMBUSTION

by Gerald Morrell and Frederick P. Povinelli

Lewis Research Center
Cleveland, Ohio

BREAKUP OF VARIOUS LIQUID JETS BY SHOCK WAVES

AND APPLICATIONS TO RESONANT COMBUSTION

By Gerald Morrell and Frederick P. Povinelli

Lewis Research Center
Cleveland, Ohio

NATIONAL AERONAUTICS AND SPACE ADMINISTRATION

BREAKUP OF VARIOUS LIQUID JETS BY SHOCK WAVES

AND APPLICATIONS TO RESONANT COMBUSTION

by Gerald Morrell and Frederick P. Povinelli

Lewis Research Center

SUMMARY

Breakup times of liquid jets in crossflow were measured in a shock tube. Three jet diameters (0.052, 0.0785, and 0.157 in.) of water, $\underline{n}$-heptane, liquid oxygen, and three glycerol-water mixtures were studied. Breakup time was found to increase regularly with an increase in the ratio of jet radius to the gas velocity behind the shock front.

A model based on mass removal from a liquid boundary layer agrees with the experimental data. A least-squares fit of measured and calculated breakup times permits quantitative estimates of breakup time or average mass removal rate for other conditions.

With atomization assumed to be the rate-controlling process, it is shown how similarity parameters of three theories of combustion resonance may be evaluated in terms of engineering design variables.

INTRODUCTION

The process of breakup and atomization, produced by shock waves acting on liquid jets or drops, may be important in oscillatory combustion either as an initiating or a driving mechanism (ref. 1). Information on the rate of this process should be helpful whether the oscillation is treated as a perturbation on the mean vaporization rate or as a detonation in a heterogeneous medium.

Although the literature on atomization is voluminous, the effects produced by shock waves have not been treated extensively. The primary interest has been in the minimum velocity for initiation of breakup (refs. 2 to 5); but from some of the pictorial sequences presented, breakup times can be inferred. Previous studies on the breakup time of water jets in shock tubes (refs. 6 and 7) indicated that mass is removed from the main body of liquid in a boundary layer for gas-stream velocities that are not too close to the minimum values required to initiate the process. In reference 7 an expression for breakup time is derived in terms of liquid and gas properties, gas stream velocity, and jet size.

The purpose of the study reported herein was to test the predicted effects

of liquid properties on breakup time. Measured breakup times of n-heptane, liquid oxygen, and three glycerol-water mixtures, along with some additional data for water, were obtained in the same apparatus that was used for a previous study. The results are correlated in terms of the boundary-layer model, and the possible significance of jet breakup in oscillatory combustion is discussed.

SYMBOLS

A	engine contraction ratio
a	constant
b	constant
L	length of liquid sheet
L'	distance from stagnation point to edge of jet
$\mathcal{L}$	heating parameter
M_o	initial mass per unit length of jet
m	fraction burned per unit length
R_o	initial jet radius
Re_o	Reynolds number based on R_o, $R_o u \rho / \mu$
r	combustor radius
t	time
t_a	action time
t_b	breakup time
t_i	chemical conversion time
t_w	wave time
u	gas velocity behind shock wave
$u_{l,av}$	arithmetic average velocity in liquid boundary layer
V	volume per unit length of jet
v_j	jet velocity
We_o	Weber number based on R_o, $\rho u^2 R_o / \sigma$

2

x distance along liquid sheet from stagnation point

δ_l thickness of liquid boundary layer

μ gas viscosity

μ_l liquid viscosity

ν kinematic viscosity, μ/ρ

ν_l liquid kinematic viscosity, μ_l/ρ_l

ρ gas density behind shock wave

ρ_l liquid density

σ interfacial tension

τ_s average pressure-sensitive time lag

χ ratio of chemical conversion time to wave time

Subscripts:

calc   calculated

exp   experimental

APPARATUS AND PROCEDURE

A schematic diagram of the apparatus is shown in figure 1. Except for the oxygen flow system, no changes were made in the arrangement described in reference 7. The square test section has an internal dimension of 2.721 inches to provide a cross-sectional area about equal to that of the 3-inch-diameter schedule 40 pipes used for the rest of the shock tube. The liquid jet is injected vertically at a station approximately 51.5 inches from the diaphragm (16.7 diam) and flows out through a 1.25-inch-diameter opening in the floor of the test section. The length of the high-pressure section could be varied from 1 inch to 8 feet to provide a range of action times from about 0.2 to 25 milliseconds. Action time is defined here as the constant-pressure period plus the time required for the pressure to decay to one-third of its initial value.

Wave speed was measured by two barium titanate blast gages located 2 feet apart, and pressure behind the wave was monitored by a strain-tube pressure transducer with a natural frequency of about 25 kilocycles and a range of 200 pounds per square inch. A sine-wave generator was used to provide a 2-kilocycle frequency for the time base. These four signals were displayed by a dual-beam oscilloscope equipped with 100-kilocycle chopping amplifiers to produce four displays on a time sharing basis.
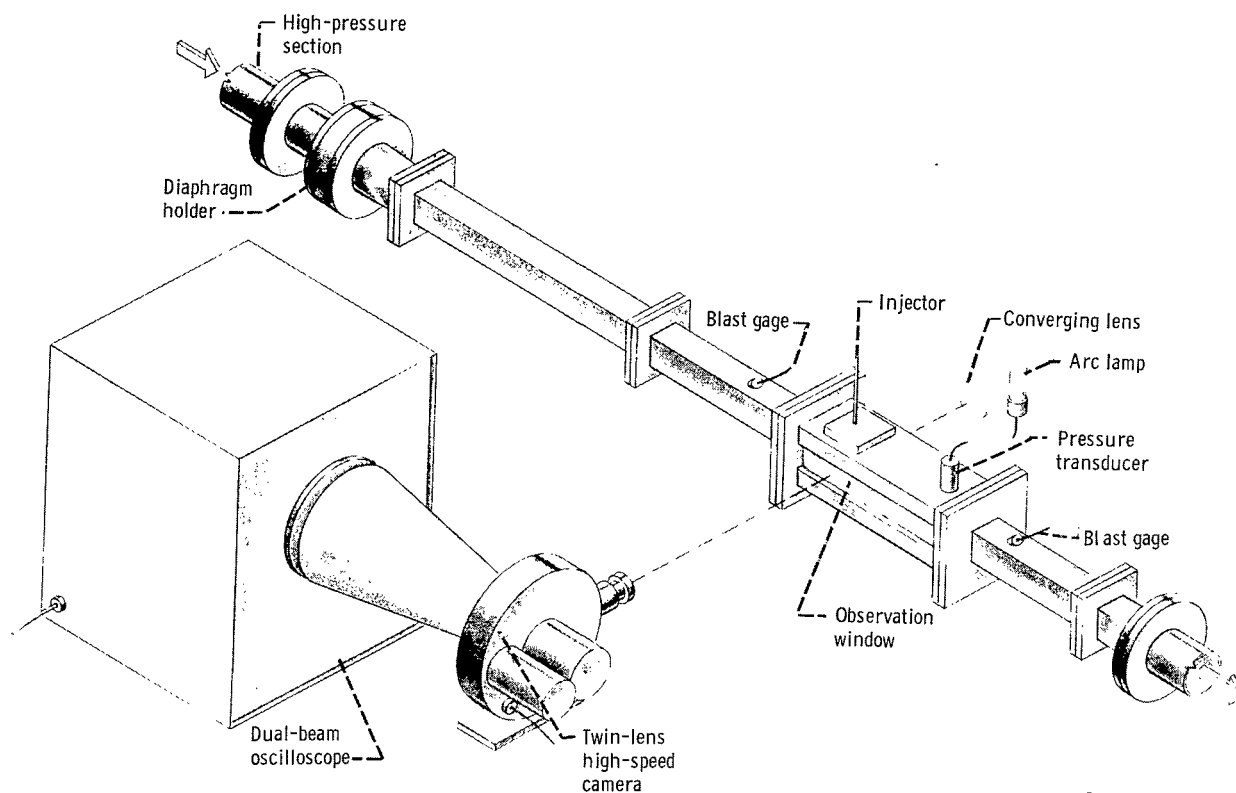
Figure I. - Schematic diagram of experimental apparatus.

Back-lighted streak photographs were taken with a 35-millimeter shutter-less high-speed camera at a film velocity of approximately 990 inches per second. The test-section window facing the camera was masked, except for an axial slit 0.1 inch wide and 14 inches long. The oscilloscope, operated in the unswept mode, was photographed simultaneously by means of a mirror arrangement to provide a real time correlation with the picture of the breakup process. A 50-millimeter $f/2$ lens was used with a demagnification of 11 at the film. A typical streak photograph is shown in figure 2 together with a corresponding framing photograph for reference.

The initial pressure in the test section was 1 atmosphere, and four nominal values of initial pressure ratio (across the diaphragm) were used. These values, together with the diaphragm materials, are shown in the table at the left. The initial

Initial pressure ratio	Nominal shock Mach number at 70° F	Diaphragm material	Diaphragm thickness, in.
1.68	1.115	Oiled onion-skin paper	Two sheets
2.63	1.225	Soft brass	0.0015
7.12	1.506	Soft brass	.004
14.61	1.725	Spring brass	.007

CD-7542

4

(a) Film strip.

(b) Streak photograph.

CS-25394

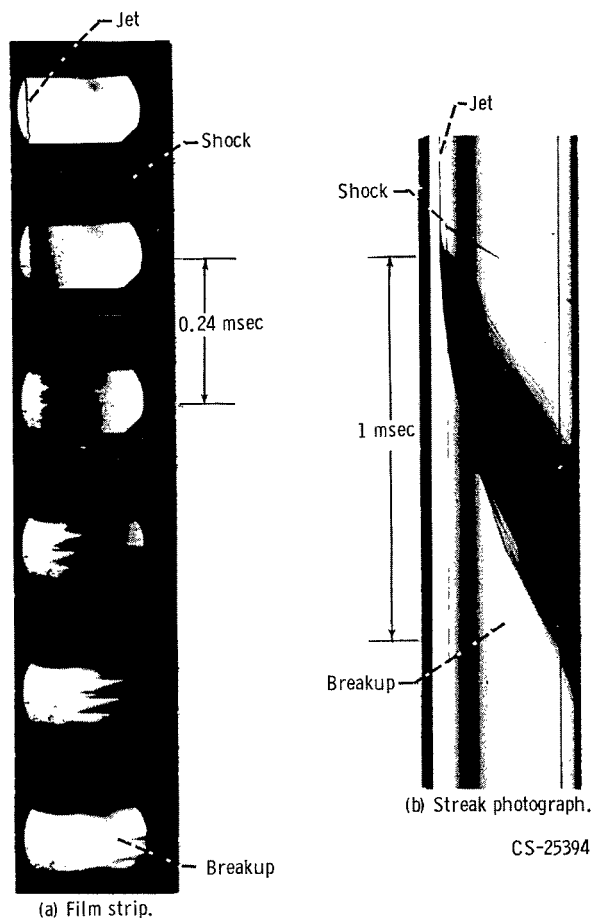Figure 2. – Typical photographs of jet breakup. Shock velocity, 1655±5 feet per second; gas velocity, 732±5 feet per second; jet diameter, 0.052 inch; breakup time, approximately, 1.1 milliseconds.

Liquid	Surface tension, lb/sec	Density, lb/cu ft	Viscosity, lb/(ft)(sec)
Water	0.161	62.4	6.72×10^{-4}
Heptane	.045	42.6	2.745×10^{-4}
Oxygen	.033	73.2	1.5×10^{-4}
15 Weight percent glycerol	.160	64.5	9.9×10^{-4}
58 Weight percent glycerol	.151	71.4	6.15×10^{-3}
79 Weight percent glycerol	.147	75.0	3.49×10^{-2}

pressures were about 90 percent of the diaphragm break pressure. The shock wave was initiated by puncturing the the diaphragm.

Gas velocity and density behind the shock wave were calculated from the measured value of shock velocity by using the one-dimensional wave equations (ref. 8) at a temperature of 70° F. The laboratory temperature was 70°±5° F. Initial air density was taken as 0.07488 pound per cubic foot, and air viscosity was assumed to be constant at 1.205×10^{-5} pound per foot per second.

Three jet diameters, 0.052, 0.0785, and 0.157 inch, were used with each of the following liquids: water, n-heptane, oxygen, and three glycerol-water mixtures. Length-to-diameter ratios of the liquid-injection orifices were at least 10, so that the jet was turbulent. In a previous study (ref. 7), no significant difference in breakup characteristics was observed between turbulent jets and smooth jets produced by a sharp-edged orifice. With the exception of oxygen, all liquids were used at 70° F. The oxygen was passed through a liquid-nitrogen heat exchanger and then through a vacuum-jacketed line to the injector. Properties of the liquids used for computation of breakup time are given in the table at the left. The oxygen properties were taken for a temperature midway between the normal boiling points of oxygen and nitrogen. In this region, the properties are quite sensitive to temperature.

RESULTS AND DISCUSSION

All the experimentally determined breakup times are plotted in figure 3 as a function of the ratio
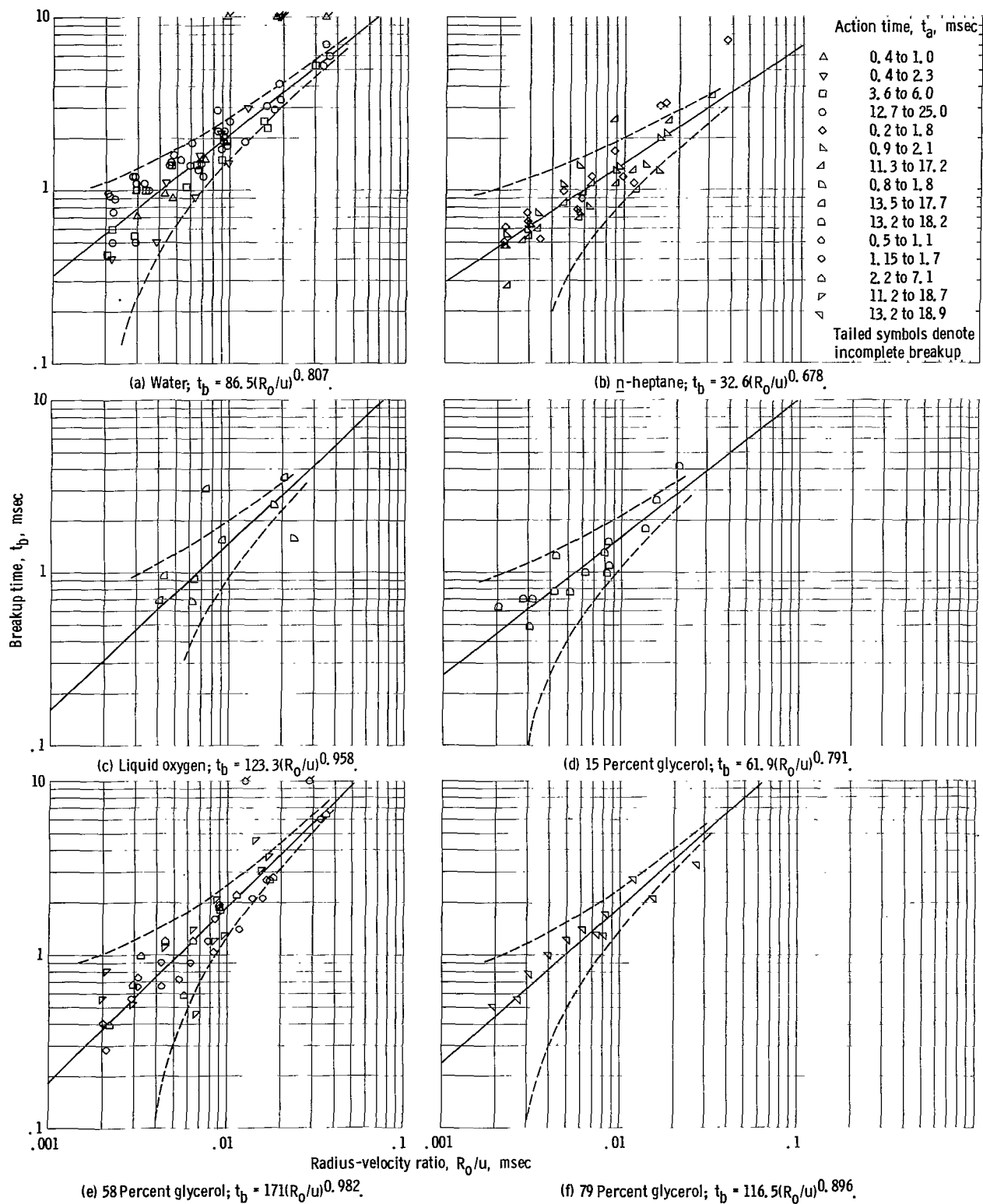
5

Figure 3. – Breakup times of jets as function of radius-velocity ratio.

(a) Water; $t_b = 86.5(R_0/u)^{0.807}$.

(b) n-heptane; $t_b = 32.6(R_0/u)^{0.678}$.

(c) Liquid oxygen; $t_b = 123.3(R_0/u)^{0.958}$.

(d) 15 Percent glycerol; $t_b = 61.9(R_0/u)^{0.791}$.

(e) 58 Percent glycerol; $t_b = 171(R_0/u)^{0.982}$.

(f) 79 Percent glycerol; $t_b = 116.5(R_0/u)^{0.896}$.

Breakup time, t_b, msec

Radius-velocity ratio, R_0/u, msec

Action time, t_a, msec

Symbol	Range
△	0.4 to 1.0
▽	0.4 to 2.3
▱	3.6 to 6.0
○	12.7 to 25.0
◇	0.2 to 1.8
◺	0.9 to 2.1
◿	11.3 to 17.2
◱	0.8 to 1.8
◲	13.5 to 17.7
▢	13.2 to 18.2
◇	0.5 to 1.1
○	1.15 to 1.7
△	2.2 to 7.1
▷	11.2 to 18.7
◁	13.2 to 18.9

Tailed symbols denote incomplete breakup

6

of initial jet radius to gas velocity behind the shock wave. In figure 3(a), data from reference 7 are also included. The solid lines represent the least-squares fit, which is of the form $t = a(R_O/u)^b$; the dashed lines bound the 99.7 percent probability region. Although a few of the data points lie outside this region and could be discarded on statistical grounds, there were no apparent discrepancies in the experiments that would justify their exclusion. The probable error was approximately 0.12 millisecond, but varied somewhat among the fluids. No systematic independent effects of R_O and u were observed. In every case of incomplete breakup, the action time was considerably less than the expected breakup time (figs. 3(a) and (e)). Incomplete breakup was the only observed effect of action time on the breakup process. In some cases, breakup times in excess of the action time were measured, which would indicate that, if the breakup process is sufficiently advanced, disintegration of the liquid phase may continue because of its inertia even in the absence of an applied stress.

In reference 7 it is shown that a model based on the formation of a liquid sheet with mass removal from the boundary layers on both sides gives reasonable agreement with the observed data for water. The volumetric removal rate may be written

$$- \frac{dV}{dt} = (2\delta_l u_{l,av})_{x=L} \tag{1}$$

where δ_l and $u_{l,av}$ are both functions of x. With L and the free-stream velocity assumed constant, equation (1) may be integrated to yield (ref. 7)

$$t_b = 0.54 \left(\frac{\rho_l}{\rho} \right)^{2/3} \left(\frac{\mu}{\mu_l} \right)^{1/3} \frac{R_O}{u} \sqrt{\frac{Re_O}{L/2R_O}} \tag{2}$$

The apparent length of the liquid sheet observed in these experiments could not be related to a simple function of Weber number and Reynolds number as was the case for water alone (ref. 7). A dimensional analysis and a least-squares fit of the data obtained with the longest action times yield the following expression:

$$\frac{L}{2R_O} = 1 + 8.23 \times 10^{-3} (Re_O)^{0.418} (We_O)^{0.340} \left(\frac{\nu}{\nu_l} \right)^{0.143} \tag{3}$$

which represents the experimental data with a probable error of 0.435.

In terms of the parameters actually varied in establishing equation (3),

$$\frac{L}{2R_O} - 1 \propto \frac{R_O^{0.76} u^{1.1} \rho^{0.615} \rho_2^{0.143}}{\sigma^{0.34} \mu_l^{0.143}}$$

By comparison, the corresponding expression of reference 7 for the parameters that actually varied in that study is

$$\frac{L}{2R_O} - 1 \propto R_O^{0.5} u^{1.5} \rho^{0.5}$$

It is seen that, although the magnitudes of the respective exponents are different, the two expressions show similar trends with respect to dependence on R_O, u, and ρ.

In reference 9 it is shown, however, that the assumption of a flat sheet of liquid is untenable. Two-dimensional photographs indicate that a liquid jet in crossflow tends to deform so as to approximate a segment of a larger cylinder. If the cross section is assumed to be a circular segment (as shown in fig. 4), the surface length can be calculated from the apparent length (altitude of the segment) for an included angle of $2\pi/3$ corresponding to the position where the dynamic pressure on the cylinder in crossflow is a minimum. The resulting expression for the corrected length is L' = 2.09 L. Substitution of the corrected equation (3) in equation (2) yields the expression

$$t_b = 0.37 \left(\frac{\rho_l}{\rho}\right)^{1/3} \left(\frac{\nu}{\nu_l}\right)^{1/3} \frac{R_O}{u} \sqrt{\frac{Re_O}{1 + 8.23 \times 10^{-3} (Re_O)^{0.418} (We_O)^{0.340} \left(\frac{\nu}{\nu_l}\right)^{0.143}}} \quad (4)$$

The average rate of breakup is given by

$$\frac{M_O}{t_b} = 8.5 \left(\frac{\rho}{\rho_l}\right)^{1/3} \left(\frac{\nu}{\nu_l}\right)^{1/6} \sqrt{\rho_l \mu_l u R_O \left[1 + 8.23 \times 10^{-3} (Re_O)^{0.418} (We_O)^{0.340} \left(\frac{\nu}{\nu_l}\right)^{0.143}\right]}$$

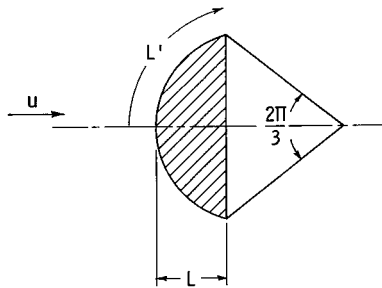In figure 5 the measured values of breakup time are plotted against the values
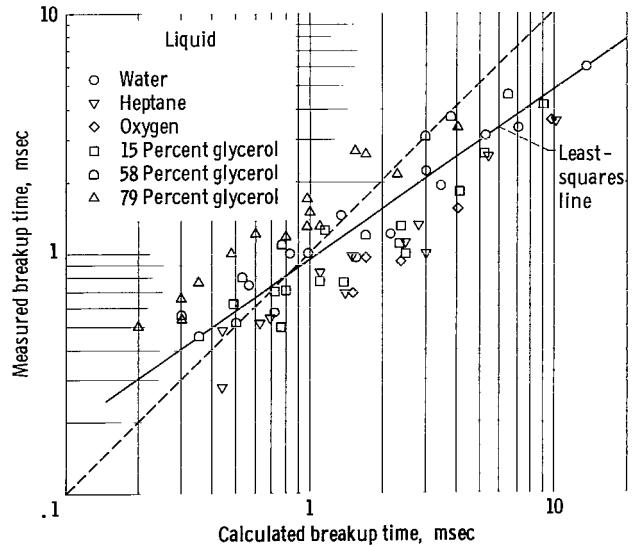

Figure 4. - Cross section of deformed jet.

Figure 5. - Comparison of measured breakup times with values calculated from equation (4).

8

computed from equation (4). The dashed line is the trend for equivalence of measured and calculated times. The calculated values tend to be high for long breakup times and somewhat low for the shortest breakup time, especially for the most viscous fluids. The measured times for liquid oxygen are all lower than the predicted times, an effect which could be due to rapid vaporization of the deforming mass.

It is also apparent that the data for the higher viscosity fluids seem to be separate from the data for the lower viscosity fluids, especially in the region of low breakup times; thus the effect of fluid viscosity on $L/2R_o$ has not accounted entirely for its influence on breakup time. It may be that the velocity profile in the liquid-phase boundary layer is also influenced by viscosity in some way. The solid line in figure 5 is the least-squares fit represented by the empirical equation

$$t_{b,exp} = 0.96\ t_{b,calc}^{0.66} \tag{5}$$

where the times are in milliseconds and $t_{b,calc}$ is obtained from equation (4).

APPLICATION TO COMBUSTION INSTABILITY

In reference 10, Penner has proposed that in order to maintain combustion stability in scaling from one rocket engine size to another, the ratio of chemical conversion time to wave time should be held constant; that is,

$$X \equiv \frac{t_i}{t_w} = constant$$

If it is assumed that the atomized liquid produced by the shock wave is rapidly burned as compared with the rate at which it is produced, t_i may be equated with t_b. For the transverse acoustic mode, $t_w \propto r$. If the flow conditions are such that

$$8.23 \times 10^{-3} (Re_o)^{0.418} (We_o)^{0.340} \left(\frac{\nu}{\nu_l}\right)^{0.143} \ll 1$$

the parametric dependence of t_b on the experimental variables is given, from equations (4) and (5), by

$$t_b \propto \frac{R_o^{0.99}}{u^{0.33}} \frac{\rho_2^{0.44}}{\rho^{0.11}} \frac{\mu^{-0.11}}{\mu_l^{0.22}}$$

If, on the other hand,

$$8.23 \times 10^{-3} (Re_o)^{0.418} (We_o)^{0.340} \left(\frac{\nu}{\nu_l}\right)^{0.143} \gg 1$$

the parametric dependence is given by

$$t_b \propto \frac{R_o^{0.74}}{u^{0.69}} \frac{\rho_l^{0.4}}{\rho^{0.32}} \frac{\mu^{-0.02}}{\mu_l^{0.17}} \sigma^{0.11} \tag{6}$$

Expression (6) appears to be more nearly applicable to rocket combustors. Substitution of expression (6) in the equation for χ yields, for a given liquid,

$$\chi \propto \frac{R_o^{0.74}}{ru^{0.69}\rho^{0.32}} = \text{constant} \tag{7}$$

For a given magnitude of perturbation u, the jet size should be scaled approximately as the 4/3 power of the combustor radius and the square root of the pressure. Equation (7) also indicates that, if an engine is scaled to a larger size while certain values of R_o and ρ are retained, the perturbation velocity must be decreased proportionally in order to retain similarity with respect to combustion stability. It appears, therefore, that the simplest method that will retain similarity with respect to combustion efficiency in combustor scale-up will tend to destabilize the system.

In reference 11, Crocco has derived, by an entirely different approach, the parameter τ_s/t_w, which must lie outside certain limits in order to achieve stability. Obviously, if the same assumption is made about the relation between τ_s and t_b as was made with respect to t_i, the conclusions will be the same as those derived from the chemical conversion parameter. In this case, however, there is a second factor that must be considered, the pressure interaction index. This pressure interaction index appears to be less sensitive to combustor size than τ_s.

A nonlinear solution for the transverse acoustic mode of oscillation is given in reference 12. For a vaporization-limited model, two parameters should be held constant in scaling to retain stability, the Mach number of the gas phase relative to the liquid phase and a heating-rate number

$$\mathcal{L} \equiv \frac{rm}{A}$$

If it is assumed that the value of m is determined by the atomization rate (i.e., atomized drops vaporize quickly compared with the rate at which they are produced), then the rate may be written (ref. 1)

$$m \propto \frac{1}{t_b v_j}$$

and

$$\mathcal{L} \equiv \frac{rm}{A} \propto \frac{r}{t_b v_j A}$$

For a given liquid, substitution of equation (5) yields

$$\mathcal{L} \propto \frac{r u^{0.69} \rho^{0.32}}{R_o^{0.74} v_j A} = \text{constant}$$

In this case, R_o, v_j, or both, must be increased to maintain similarity with respect to system stability as combustor size and pressure are increased.

All three theories of combustion instability are consistent in showing that similarity with respect to stability cannot be maintained in scaling up combustor size or pressure if the injection characteristics remain invariant. For a single-stage combustor, however, injection invariance is required to maintain similarity with respect to combustor efficiency (ref. 13). The two requirements, therefore, are incompatible in a straightforward scale-up. It might be possible to overcome the impasse by properly staging the injection process. In this case, modeling experiments could be conducted on the individual stages, but the matching problems would be deferred to the full-scale test program.

SUMMARY OF RESULTS

Breakup times in a transverse gas flow have been measured in a shock tube for three sizes of jets of water, n-heptane, liquid oxygen, and three glycerol-water mixtures. In all cases the breakup time was found to increase regularly with the ratio of initial jet radius to gas velocity behind the shock wave.

A model based on mass removal from a liquid boundary layer gives fair agreement with the observed values of breakup time. The model tends to give high values in the range of long breakup times (>3 msec) and tends to give low values for shorter breakup times (<1 msec), especially for the more viscous liquids. An empirical equation was derived on the basis of a least-squares fit of measured to calculated breakup times.

With liquid breakup assumed to be the rate-controlling process, it was shown how similarity parameters for three combustion instability theories could be evaluated.

The three theories are consistent in showing that, when all other factors are held constant, jet radius should be scaled in proportion to the 4/3 power of the combustor radius and the square root of the combustion pressure in order to maintain similarity with respect to stability. They are consistent, furthermore, in showing that scale-up without change in injector radius or jet velocity will reduce stability, since a smaller value of perturbation velocity is required to maintain similarity.

Lewis Research Center
 National Aeronautics and Space Administration
  Cleveland, Ohio, April 8, 1964

REFERENCES

1. Priem, R. J., and Morrell, G.: Application of Similarity Parameters for Correlating High-Frequency Instability Behavior of Liquid Propellant Combustors. Vol. 6 of Prog. in Astronautics and Rocketry, Academic Press, 1962, p. 305.

2. Lane, W. R.: Shatter of Drops in Streams of Air. Ind. and Eng. Chem., vol. 43, no. 6, June 1951, pp. 1312-1317.

3. Engel, O. G.: Fragmentation of Waterdrops in the Zone Behind an Air Shock. Jour. Res. Nat. Bur. Standards, vol. 60, no. 3, Mar. 1958, p. 245.

4. Muirhead, J. C.: Blast Wave Attenuation. Pt. I. Water Walls. Suffield Tech. Paper 175, Defence Research Board (Canada), 1959.

5. Hanson, A. R., Domich, E. G., and Adams, H. S.: Shock Tube Investigation of the Breakup of Drops by Air Blasts. Phys. of Fluids, vol. 6, no. 8, Aug. 1963, pp. 1070-1080.

6. Morrell, G.: Breakup of Liquid Jets by Transverse Shocks. Eighth Symposium (International) on Combustion, The Williams & Wilkins Co., 1962, p. 1059.

7. Morrell, Gerald: Rate of Liquid Jet Breakup by a Transverse Shock Wave. NASA TN D-1728, 1963.

8. Ames Research Staff: Equations, Tables, and Charts for Compressible Flow. NACA TR 1135, 1953. (Supersedes NACA TN 1428.)

9. Clark, Bruce J.: Breakup of a Liquid Jet in a Transverse Flow of Gas. NASA TN D-2424, 1964.

10. Penner, S. S.: On the Development of Rational Scaling Procedures for Liquid-Fuel Rocket Engines. Jet Prop., vol. 27, no. 2, pt. 1, Feb. 1957, pp. 156-161.

11. Crocco, L., and Cheng, Sin I.: Theory of Combustion Instability in Liquid Propellant Rocket Motors. Agardograph 8, Butterworths Sci. Pub. (London), 1956, p. 86.

12. Priem, Richard J., and Guentert, Donald C.: Combustion Instability Limits Determined by a Nonlinear Theory and a One-Dimensional Model. NASA TN D-1409, 1962.

13. Priem, Richard J., and Heidmann, Marcus F.: Propellant Vaporization as a Design Criterion for Rocket-Engine Combustion Chambers. NASA TR R-67, 1960. (Supersedes NASA TN's 3883, 3985, 4098, and 4219.)

NASA SCIENTIFIC AND TECHNICAL PUBLICATIONS

TECHNICAL REPORTS: Scientific and technical information considered important, complete, and a lasting contribution to existing knowledge.

TECHNICAL NOTES: Information less broad in scope but nevertheless of importance as a contribution to existing knowledge.

TECHNICAL MEMORANDUMS: Information receiving limited distribution because of preliminary data, security classification, or other reasons.

CONTRACTOR REPORTS: Technical information generated in connection with a NASA contract or grant and released under NASA auspices.

TECHNICAL TRANSLATIONS: Information published in a foreign language considered to merit NASA distribution in English.

TECHNICAL REPRINTS: Information derived from NASA activities and initially published in the form of journal articles.

SPECIAL PUBLICATIONS: Information derived from or of value to NASA activities but not necessarily reporting the results of individual NASA-programmed scientific efforts. Publications include conference proceedings, monographs, data compilations, handbooks, sourcebooks, and special bibliographies.

Details on the availability of these publications may be obtained from:

SCIENTIFIC AND TECHNICAL INFORMATION DIVISION

NATIONAL AERONAUTICS AND SPACE ADMINISTRATION

Washington, D.C. 20546